Cerebral Cortex March 2010;20:704–719
doi:10.1093/cercor/bhp136
Advance Access publication July 24, 2009

Forelimb Muscle Representations and Output Properties of Motor Areas in the Mesial Wall of Rhesus Macaques

Marie-Hélène Boudrias[1,3], Sang-Pil Lee[1,2], Stan Svojanovsky[1] and Paul D. Cheney[1]

[1]Department of Molecular & Integrative Physiology, University of Kansas Medical Center (KUMC), Kansas City, KS 66160, USA, [2]Hoglund Brain Imaging Center, University of Kansas Medical Center, Kansas City, KS 66160, USA and [3]Current address: Sobell Department of Motor Neuroscience and Movement Disorders, Institute of Neurology, University College London, Queen Square, London WC1N 3BG, UK

In this study, forelimb organizations and output properties of the supplementary motor area (SMA) and the dorsal cingulate motor area (CMAd) were assessed and compared with primary motor cortex (M1). Stimulus-triggered averages of electromyographic activity from 24 muscles of the forelimb were computed from layer V sites of 2 rhesus monkeys performing a reach-to-grasp task. No clear segregation of the forelimb representation of proximal and distal muscles was found in SMA. In CMAd, sites producing poststimulus effects in proximal muscles tended to be located caudal to distal muscle sites, although the number of effects was limited. For both SMA and CMAd, facilitation effects were more prevalent in distal than in proximal muscles. At an intensity of 60 μA, the mean latencies of M1 facilitation effects were 8 and 12.1 ms shorter and the magnitudes ~10 times greater than those from SMA and CMAd. Our results show that corticospinal neurons in SMA and CMAd provide relatively weak input to spinal motoneurons compared with the robust effects from M1. However, a small number of facilitation effects from SMA and CMAd had latencies as short as the shortest ones from M1 suggesting a minimum linkage to motoneurons as direct as that from M1.

Keywords: corticospinal neuron, EMG, forelimb, motor control, primate, supplementary motor area

Introduction

Penfield and Welch (1951) and Woolsey et al. (1952), using electrical stimulation of the cortical surface, demonstrated the existence of a motor area on the medial wall of the hemisphere in monkeys, which they termed the supplementary motor area (SMA). Since its discovery, more recent studies have shown that the previously described SMA contains multiple motor areas, each one with its own set of corticospinal neurons. In addition to SMA, 3 cingulate motor areas have been identified in the cingulate sulcus including the dorsal cingulate motor area (CMAd), the ventral cingulate motor area, and the rostral cingulate motor area (Dum and Strick 1991; Luppino et al. 1991; Matelli et al. 1991; Galea and Darian-Smith 1994; He et al. 1995). More significantly, SMA and CMAd contain substantial numbers of corticospinal neurons projecting to the spinal cord where they can potentially influence motoneurons via pathways independent of the primary motor cortex (M1) (Dum and Strick 1991; Galea and Darian-Smith 1994).

M1 corticospinal neurons have been shown to terminate not only in the intermediate zone of the spinal cord but also in the ventral horn with some of the terminations making direct connections with spinal motoneurons (Kuypers 1981; Porter and Lemon 1993). Such monosynaptic connections between corticospinal neurons and motoneurons have been regarded as a prerequisite for the generation of independent finger movements (Porter and Lemon 1993). Several anatomical studies have provided evidence supporting a direct role of SMA and CMAd in the control of hand movements, paralleling that of M1. Using anterograde tracers to examine the spinal pattern of terminations of corticospinal neurons from SMA and CMAd, it was demonstrated that even if less numerous than in M1, both have terminations in the ventral horn, particularly on motoneuron pools involved in the generation of finger and wrist movements (Dum and Strick 1996). Moreover, SMA's terminations were shown to be located in close proximity to retrogradely labeled motoneurons (Rouiller et al. 1996). Based on intracellular recording from 84 upper limb motoneurons, Maier et al. (2002) found excitatory postsynaptic potentials (EPSPs) at monosynaptic latencies relative to the I wave of the descending volley evoked from stimulation of SMA. However, the monosynaptic connections from M1 were far more numerous and stronger than those from SMA. Nevertheless, these findings suggest that a least some corticospinal neurons in SMA could have an output efficacy similar to M1 corticospinal neurons.

Although the number and location of the corticospinal neurons contained in SMA and CMAd have been described in detail, disparities exist in descriptions of their forelimb organization. The topographic organization of SMA and CMAd examined by injecting retrograde tracers in cervical segments of the spinal cord showed segregated zones of proximal and distal representation of corticospinal neurons in each area (Dum and Strick 1991; He et al. 1995). In contrast, the few studies that have used intracortical microstimulation (ICMS) to investigate forelimb movements from SMA reported no clear segregation between proximal and distal forelimb representations (Macpherson JM et al. 1982; Mitz and Wise 1987; Luppino et al. 1991).

ICMS-evoked forelimb movements have also been reported from CMAd (Luppino et al. 1991; Akazawa et al. 2000; Takada et al. 2001; Akkal et al. 2002), in agreement with the presence of corticospinal terminations in cervical segments of the spinal cord (He et al. 1995). Based on tracer studies, He et al. (1995) reported that proximal and distal corticospinal neurons in CMAd were segregated with a greater number of neurons representing distal muscles. However, the motor output properties of CMAd based on stimulation have not been fully established.

Stimulus-triggered averaging (StTA) of electromyographic (EMG) activity gives the sign of synaptic output to motoneurons (excitation or inhibition) and enables quantitation of the latency and magnitude of motor output from small clusters of corticospinal neurons to any number of recorded muscles. Using this technique, the existence of segregated proximal and

distal muscle representations were demonstrated in the forelimb area of M1 (Park et al. 2001). Therefore, one of the main goals of this study was to use StTA of EMG activity to further investigate the organization of SMA and CMAd in terms of proximal and distal forelimb muscle representations.

The second goal of this study was to evaluate the efficacy of motor output from SMA and CMAd in relation to M1. The data presented build upon work previously reported from our laboratory on SMA (Boudrias et al. 2006). We have now studied a substantially larger number of sites in SMA to investigate in greater detail the forelimb organization and have extended the study to include CMAd and M1. We used the same parameters of stimulation (current intensity of 60 μA) for sites in all 3 areas (SMA, CMAd, and M1) for direct comparison of their motor outputs. We also restricted our data set to sites located in or near layer V of the cortical gray matter. The fact that SMA, CMAd, and M1 contain comparable densities of corticospinal neurons suggests that the same parameters of stimulation applied to each of these areas might activate a similar number of corticospinal neurons (Dum and Strick 1991). Accordingly, applying StTA of EMG activity at the same intensity to SMA, CMAd, and M1 was intended to provide a measure of motor output efficacy that would be directly comparable across cortical areas.

Materials and Methods

Behavioral Task and Surgical Procedures

Data were collected from 2 male rhesus monkeys (*Macaca mulatta*, 8–10 kg, 5 and 8 years of age) trained to perform a reach-to-grasp task as described in previous studies (Belhaj-Saif et al. 1998; McKiernan et al. 1998). The monkey initiated the task by placing its right hand on a pressure plate for a preprogrammed length of time. This triggered the release of a food pellet. The monkey then reached and grasped the pellet, brought it to its mouth, and completed the task by returning its hand to the pressure plate. This task was chosen because it required the coactivation of multiple proximal and distal forelimb muscles in natural and functional synergies.

The animals were identified as monkey J and monkey Y and will be referred to as such throughout the report. On completion of training, a recording chamber was implanted over the left hemisphere of each monkey, allowing the exploration of a cortical area 30 mm in diameter providing full access to the forelimb areas of SMA, CMAd, and M1 (Figs. 1 and 2). The chambers were stereotaxically implanted at anterior 12.9 mm, lateral 9 mm (monkey Y), and at anterior 20.9 mm, lateral 12.9 mm (monkey J) with an angle of 15 deg to the midsagittal plane.

EMG activity was recorded from 24 muscles of the forelimb, as described previously by Park et al. (2000). Monkey J was implanted using a modular subcutaneous implant technique and monkey Y was implanted using a cranial implant technique. In the case of the modular implant method (monkey J), at all times other than recording sessions, the monkey wore a jacket reinforced with stainless steel mesh to protect the EMG implant. For each monkey, muscles were implanted with a pair of multi-stranded stainless steel wires (Cooner Wire AS632) led subcutaneously to connectors on the forearm (modular implant), or to a connector anchored to the dental acrylic mound, next to the recording chamber (cranial implant). EMGs were recorded from 5 shoulder muscles: pectoralis major (PEC), anterior deltoid (ADE), posterior deltoid (PDE), teres major (TMAJ), and latissimus dorsi (LAT); 7 elbow muscles: biceps short head (BIS), biceps long head (BIL), brachialis (BRA), brachioradialis (BR), triceps long head (TLON), triceps lateral head (TLAT), and dorso-epitrochlearis (DE); 5 wrist muscles: extensor carpi radialis (ECR), extensor carpi ulnaris (ECU), flexor carpi radialis (FCR), flexor carpi ulnaris (FCU), and palmaris longus (PL); 5 digit muscles: extensor digitorum communis (EDC), extensor digitorum 2 and 3 (ED 2,3), extensor digitorum 4 and 5 (ED 4,5), flexor digitorum superficialis (FDS), and flexor digitorum profundus (FDP); and 2 intrinsic hand muscles: abductor pollicis brevis (APB) and first dorsal interosseus (FDI). For monkey Y, 1 lead of TLON and TLAT was combined to form 1 triceps muscle (TRI) recording. One lead of APB and FDI was also combined to form an intrinsic hand muscle (Intrins.) recording. This was necessary because one lead of each pair was high impedance. Shoulder and elbow muscles are considered proximal muscles and wrist, digit, and intrinsic hand muscles are considered distal muscles throughout the paper.

EMG recordings were tested for cross-talk by computing EMG-triggered averages. Muscles showing cross-talk were eliminated from the data base. For monkey Y, BR, FCU, and ED 4,5 and for monkey J, BR for one implant and FDS in another implant showed cross-talk and were rejected from the analysis. In normalizing for the different number of muscles recorded at each joint, intrinsic hand (Intrins.) and triceps (TRI) muscles for monkey Y were each considered to be 2 muscles because either of the combined muscles could have been the origin of a poststimulus effect (PStE). All surgeries were performed under deep general anesthesia and sterile conditions. Analgesic and antibiotic drugs were given postoperatively in accordance with the Association for Assessment and Accreditation of Laboratory Animal Care and the Guide for the Care and Use of Laboratory Animals, published by the US Department of Health and Human Services and the National Institutes of Health.

Data Recording

Stimuli were applied to SMA, CMAd, and M1, and recorded together with EMG signals, while the monkey performed a reach-to-grasp task. Electrode penetrations are summarized and represented in Table 1 and Figure 1. Penetrations were performed in a random spatial order using a 1-mm grid throughout the mesial wall of SMA's forelimb representation in each animal. In some areas, electrode tracks were placed 0.5 mm from each other or in the center of the 1-mm square formed by 4 adjacent tracks to achieve greater spatial resolution. Penetrations in CMAd were made using a 1-mm grid or less. In monkey J, the lateral boundary of SMA was sampled using a 2-mm spacing. An area of up to 7 mm lateral to the midline and 13 mm along the antero-posterior axis of the lateral aspect of the hemisphere for each animal was covered with electrode penetrations. Sites located at or below 6.5 mm from the cortical surface were not included in the SMA database; such sites were either rejected or considered to be part of CMAd. The bulk of the forelimb representation of SMA where PStEs were obtained covered an area about 7–8 mm rostro-caudally and 3 mm medio-laterally from the midline on the lateral aspect of the hemisphere.

Penetrations in M1 were randomly selected within the forelimb representation and systematically stimulated at 2 different intensities, 15 and 60 μA (Table 2 and Fig. 1). The use of 15 μA is based on previous StTA studies in which it was found that this specific intensity of stimulation was optimal to map and assess M1 output properties (Park et al. 2001, 2004). A total of 30 tracks were selected in M1 from the 2 monkeys. Half of the penetrations were performed on the anterior part of M1 (surface part) and the other half were performed on the posterior part of M1 (anterior bank of the precentral gyrus). Compared with the number of muscles showing PStEs from M1 at 15 μA, at 60 μA, the number of muscles with PStEs increased substantially (Fig. 6). However, for purposes of quantifying the change in magnitude and latency of PStEs at 15 and 60 μA, only effects present at both intensities were included in the final data set. This avoided distortion of the data set by recruitment of new PStEs at 60 μA that were weaker and longer in latency.

Glass and Mylar insulated platinum–iridium electrodes with typical initial impedances between 0.7 and 2 MΩ (Frederick Haer & Co.) were used for cortical recording and stimulation. The electrode was advanced using a manual hydraulic microdrive and stimulation was performed at 0.5-mm intervals. Measurements of depth in the cortex were referenced to first activity. Only sites in or near the cortical gray matter of layer V of SMA, CMAd, and M1 were included in this analysis. Sites corresponding to layer V were estimated using a combination of criteria including electrode depth and changes in background activity. White matter was identified by an abrupt decrease in background activity in comparison to gray matter. Because tracks were obtained at an angle of 15-deg to the midsagittal plane, distances between the

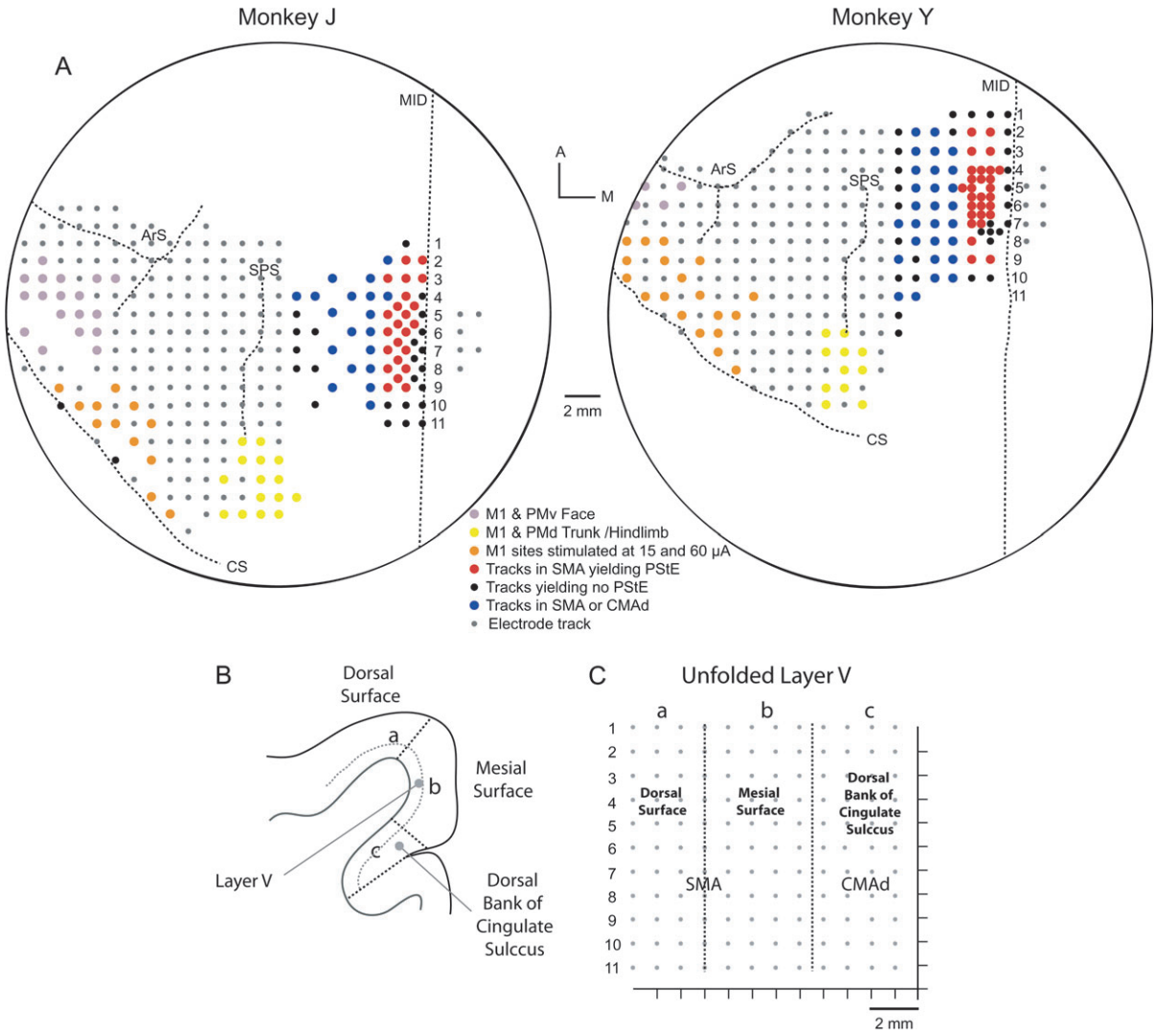

Figure 1. Reconstruction procedures applied to the mesial wall of the cortex based on MR images and electrophysiological data. (*A*) Surface view of the electrode penetration maps of the left hemisphere for both monkeys. Dotted lines indicate anatomical sulci. Abbreviations: A, Anterior; ArS, arcuate sulcus; CS, central sulcus; M, medial; MID, midline; and SPS, superior precentral sulcus. Numbers 1–11 are 1 mm apart and referenced to the coronal section represented on the unfolded layer V map in (*C*). Tracks where ICMS produced face and mouth movements in M1 and ventral premotor area (PMv) are marked by purple–pink dots; tracks where ICMS-evoked hindlimb movements in M1 are marked by yellow dots; tracks randomly selected from the M1 forelimb area for stimulation at both 15 and 60 μA are marked by orange dotes; tracks where StTA yielded PStEs from SMA are marked by red dots; tracks more lateral along the hemisphere that intersected SMA or CMAd deep along the mesial surface and produced effects are marked by blue dots; tracks where StTA did not produce PStEs are marked by small black dots; and tracks used for surface reconstruction of the brain but where data collected were not included in this analysis are marked by small gray dots; (*B*) Coronal section (Monkey J, section 1) of the mesial wall and the cortical dorsal surface of SMA based on MRI image; (*C*) Map of unfolded layer V of the gray matter of SMA and CMAd represented in 2D coordinates.

electrode's site of penetration on the lateral surface of the hemisphere and its entry into CMAd and/or penetration of the midline space (noticeable by a changes in background activity) could be calculated. These measurements were matched to those obtained from magnetic resonance imaging (MRI). For example, the frontal image of Figure 1*B* represents a section through the cortex from which cortical gray matter, white matter, and the midline could be highlighted and measured. To further aid in matching the electrode penetrations to the MR images, the dura was opened during the chamber implantation to confirm the location of the central sulcus.

Cortical unit activity and EMG activity were simultaneously monitored along with task-related signals. EMGs were filtered from 30 Hz to 1 kHz, digitized at 4 kHz, and full-wave rectified. StTAs of EMG activity (15 and 60 μA at 7–15 Hz) were computed for 19–24 muscles of the forelimb from stimuli applied throughout all phases of the reach-to-grasp task. Individual stimuli were symmetrical biphasic pulses (0.2 ms negative followed by 0.2 ms positive). All StTAs were based on a minimum of 500 or 1000 trigger events for M1 and SMA/CMAd, respectively. The number of trigger events performed in SMA and CMAd was increased in comparison to M1, in order to detect the weaker PStEs produced in these areas.

Data Analysis

Averages were compiled using an epoch of 120 ms (30-ms pretrigger to 90 ms posttrigger) for all sites in SMA and CMAd except for 15 tracks in monkey J (Fig. 1). For reasons of efficiency, shorter epochs were used for tracks located more than 3.5 mm lateral to the midline to explore cortical areas located outside of SMA where we were not concerned about detecting long latency effects. For some of these tracks, a 60-ms length epoch, extending from 20 ms before the trigger to 40 ms after the trigger was used. The analysis period of 120 ms was also used for 16 tracks in M1 to evaluate the possible presence of long latency facilitation peaks (mean onset of 55.2 ± 7.2 ms), as previously observed in SMA (Boudrias et al. 2006). In the current study, long latency facilitation peaks were also observed in SMA and at a few sites in CMAd

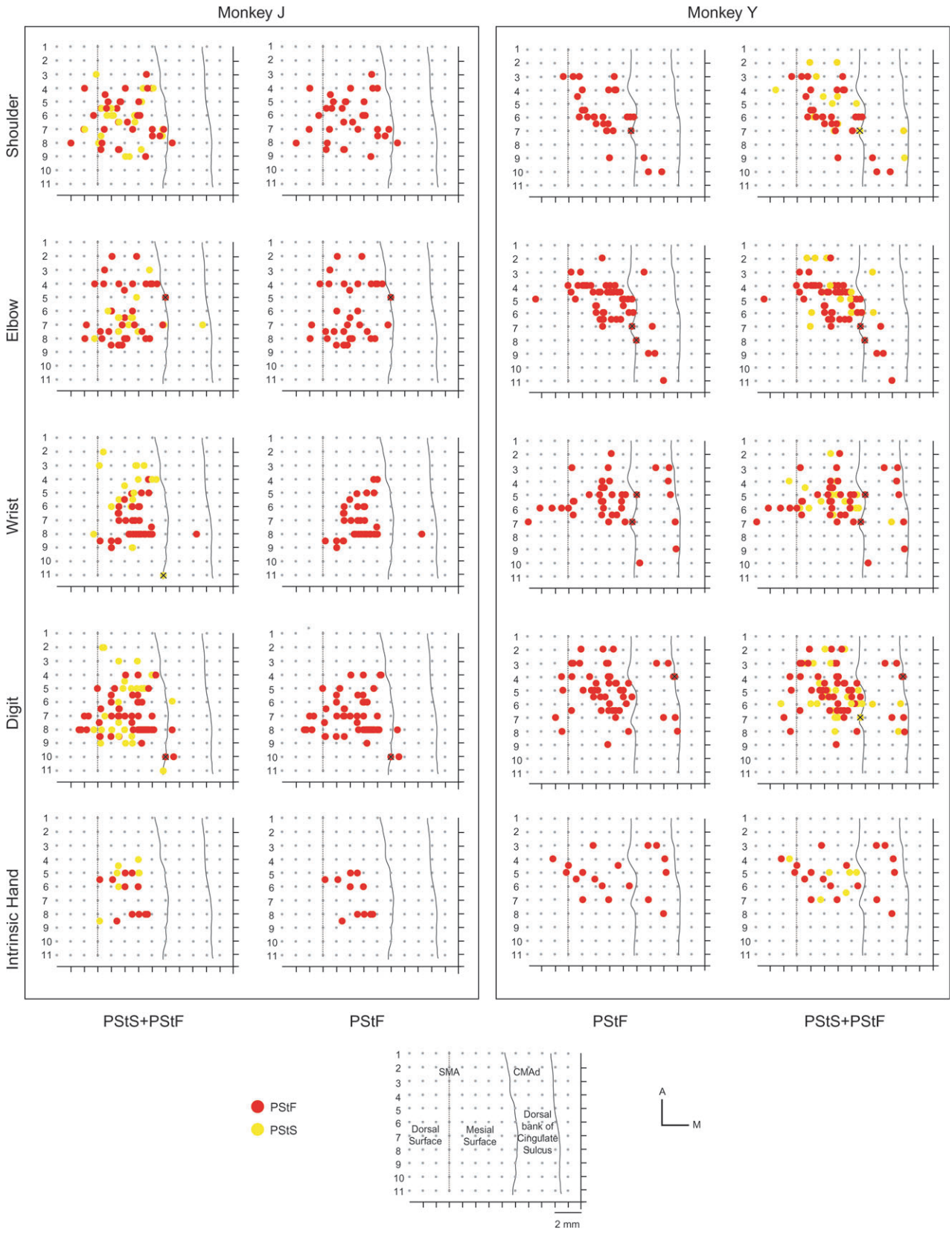

Figure 2. Two-dimensional unfolded layer V maps of the mesial wall showing the organization of PStF and PStS at each joint (shoulder, elbow, wrist, digit, and intrinsic hand) based on StTA of EMG activity at 60 μA for each monkey. The color-coded motor representation for proximal and distal joints is shown in the figure. Map unfolding procedures are explained in Materials and Methods.

Table 1
Summary of data collected from M1, SMA, and CMAd

	M1			SMA			CMAd		
	Monkey Y	Monkey J	Total	Monkey Y	Monkey J	Total	Monkey Y	Monkey J	Total
Electrode tracks	18	12	30	97	66	163	28	19	47
Sites stimulated	29	22	51	574	440	1014	81	44	125
PStF effects	200	140	340	165	176	341	27	4	31
PStS effects	1	10	11	86	86	172	10	2	12
Totals PStEs	201	150	351	243	252	513	37	6	43

Note: M1 data are based on effects that were present at both 15 and 60 μA (biphasic effects excluded).

Table 2
Latency and magnitude of PStF and PStS effects from M1, SMA, and CMAd

Facilitation	M1 @ 15 μA $N = 340$	M1 @ 60 μA $N = 340$	SMA @ 60 μA $N = 341$	CMAd @ 60 μA $N = 31$
Onset latency (ms)				
Proximal	8.2 ± 1.4	7.1 ± 1.3	16.1 ± 5.1	18.6 ± 7.0
Distal	9.1 ± 1.5	8.0 ± 0.9	15.4 ± 4.9	20.4 ± 8.3
All	8.8 ± 1.6	7.7 ± 1.2	15.7 ± 5.0	19.8 ± 8.0
Magnitudes (ppi)				
Proximal	24.1 ± 16.3	90.8 ± 63.2	14.6 ± 5.9	12.5 ± 4.3
Distal	51.7 ± 59.4	196.8 ± 155.7	15.2 ± 4.5	16.9 ± 4.9
All	41.8 ± 50.4	158.8 ± 140.1	14.9 ± 5.2	15.6 ± 5.1
Distribution				
Proximal	38%	38%	43%	27%
Distal	62%	62%	57%	73%
All PStF *	97%	97%	66%	72%
Inhibition	$N = 11$	$N = 11$	$N = 172$	$N = 12$
Onset latency (ms)				
Proximal	8.2 ± 0.8	8.8 ± 0.8	33.3 ± 8.8	35.2 ± 14.3
Distal	11.3 ± 1.2	11.6 ± 1.5	32.3 ± 8.9	35.3 ± 10.5
All	10.5 ± 1.9	10.9 ± 2.0	32.7 ± 8.9	35.3 ± 12.2
Magnitudes (ppd)				
Proximal	−19.3 ± 9.4	−28.9 ± 15.0	−12.5 ± 3.5	−10.6 ± 2.4
Distal	−16.4 ± 9.7	−27.9 ± 13.6	−18.8 ± 3.5	−13.4 ± 3.3
All	−17.2 ± 9.7	−28.6 ± 15.4	−13.3 ± 3.6	−12.2 ± 3.3
Distribution				
Proximal	26%	26%	41%	46%
Distal	74%	74%	59%	54%
All PStS *	3%	3%	34%	28%

Note: M1 data are based on effects that were present at both 15 and 60 μA. Magnitudes are expressed as ppi or ppd. *All PStF and all PStS as a percent of the total number of PStEs obtained.

but not at any of the 51 M1 sites tested. The mechanism of these late peaks is unclear and will not be discussed further in this report.

Segments of EMG activity associated with each stimulus were evaluated and accepted for averaging only when the average of all EMG data points over the entire epoch was equal to or greater than 5% of full-scale input level (± 5 V) for our data acquisition system (Power 1401, Cambridge Electronic Design Ltd). This prevented averaging segments where EMG activity was minimal or absent (McKiernan et al. 1998).

At each stimulation site, averages of EMG activity were obtained from 24 muscles. Mean baseline activity and standard deviation (SD) were measured from EMG activity in the pretrigger period (20–30 ms). StTAs were considered to have a significant poststimulus facilitation (PStF) or poststimulus suppression (PStS) if the StTA crossed a level equivalent to 2SD of the mean of the baseline EMG, for a period of time equal to or greater than 1.25 ms (5 points). The magnitudes of PStF and PStS were expressed as the peak percent increase (ppi) or peak percent decrease (ppd) in EMG activity above (facilitation) or below (suppression) baseline. Categorization of effects as either facilitation or suppression was based on the shortest latency effect. Many effects from M1 were biphasic with suppression following facilitation (see Fig. 6 for examples). Only the facilitation component of these effects was measured because of uncertainty about the onset and nature of the suppression effect. Biphasic effects were observed from all 3 cortical areas and represented 68% of effects from M1, 14% of effects from SMA, and 13% of effects from CMAd.

Statistical Analysis of Spatial Representations in SMA

Pairwise comparisons were made for data sets (maps) of facilitation effects (shoulder, elbow, wrist, digit, and intrinsic hand muscle) and for a proximal versus distal maps of SMA in each monkey (Fig. 1). Facilitation and suppression maps at the same joint were also tested against each other (Fig. 2). The Kolmogorov–Smirnov (K–S) test was used to establish whether 2 data sets (maps) were derived from the same population, regardless of their underlying distributions. We applied this nonparametric statistic to test the null hypothesis of no difference. The density of the data was established from graphical interpretation, where each measured sample point was expressed in a Cartesian coordinate system. StatMost (Statistical Analysis and Graphics, v.2.50) software was used to calculate K–S and probability values.

ICMS

Trains of repetitive ICMS were performed in SMA and M1 at those sites where no PStEs were detected, to identify the motor output representation of muscles not implanted with EMG electrodes (face, trunk, and hindlimb). ICMS consisted of a train of symmetrical biphasic stimulus pulses (0.2 ms negative followed by 0.2 ms positive) at a frequency of 330 Hz (Asanuma and Rosen 1972), a train duration of 100–500 ms, and an intensity of 30–100 μA. Evoked movements and muscle contractions detected visually were noted and recorded on videotape.

Data Analysis of MRI

MR images were obtained from a 3-T Siemens Allegra system with the monkey's head mounted in an MRI compatible stereotaxic apparatus. Structural MRIs and the reconstructed 3D image of the brain were used to guide the implantation of the recording chamber. The orientation and location of the penetrations (Fig. 1) were matched to the MRI reconstruction of the brain as described above. Based on the corresponding frontal sections of MRIs of the mesial wall, 2D maps of unfolded layer V were constructed for SMA and CMAd (Figs. 2 and 3).

Results

PStEs restricted to layer V of the forelimb representation of SMA, CMAd, and M1 were recorded from the left hemisphere in 2 monkeys. StTA of EMG activity from 24 muscles was performed in a total of 240 tracks located in SMA, CMAd, and M1 (see Table 1 for a complete description of the data collected). The cortex was explored up to 7 mm lateral to the midline. No PStEs from SMA were obtained more than 3 mm away from the midline on the lateral part of the hemisphere (red dots in Fig. 1). Because the recording chamber was at a 15-deg angle to the sagittal plane, some tracks at distances greater than 3 mm lateral to the midline intersected SMA and CMAd at sites deep along the mesial wall of the hemisphere. Tracks producing PStEs from these sites are indicated by the blue dots in Figure 1.

In SMA, movements of the mouth were evoked with ICMS at the most anterior sites (monkey Y) and hindlimb movements from the most posterior sites (monkeys J and Y). These results confirm the general somatotopic organization of SMA described by others (Mitz and Wise 1987; Luppino et al. 1991; Inase et al. 1996; Akazawa et al. 2000; Takada et al. 2001; Akkal et al. 2002). CMAd's location was extrapolated from SMA's boundaries as established previously (Dum and Strick 1991; Luppino et al. 1991; Matelli et al. 1991; He et al. 1995). ICMS also revealed a somatotopic representation of the forelimb region in M1 comparable with that reported by Park et al. (2001).

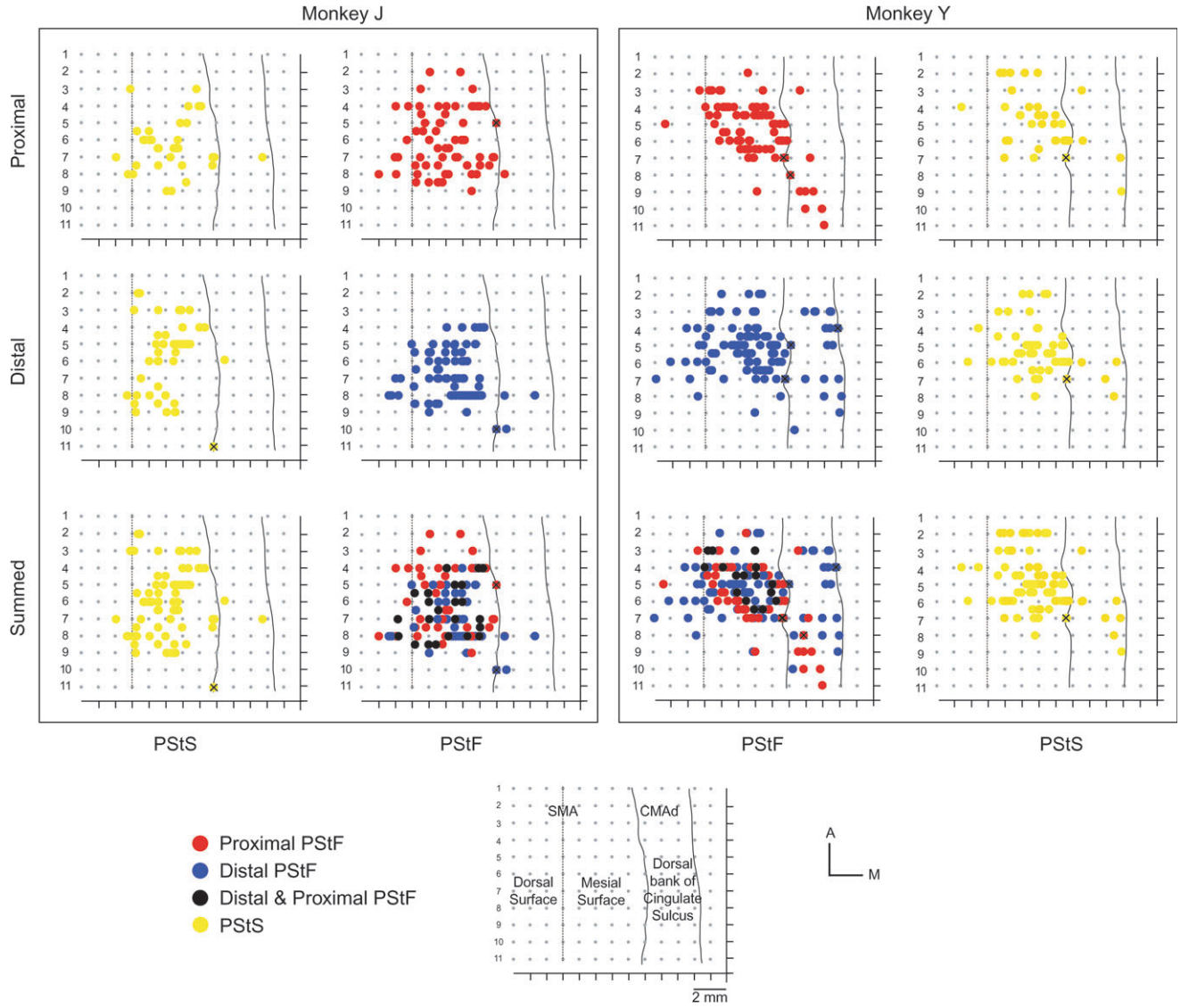

Figure 3. Maps of SMA and CMAd for 2 monkeys represented in 2D coordinates after unfolding the mesial wall of the cortex. Maps are based on PStF and PStS effects at proximal and distal joints. Effects marked with an X were not included in the SMA or CMAd data set because they were located on the border of 2 motor areas. Map unfolding procedures are explained in Materials and Methods.

Maps of SMA Based on PStEs

Comparison of 2D unfolded layer V maps of SMA revealed no significant segregation in the representation of joint-based muscle groups (K–S, $P > 0.05$) (Fig. 2). In both monkeys, we observed an area with a large number of PStEs in distal muscles. This area was localized in the posterior part of SMA at a particular depth in the mesial wall (Figs. 2 and 3, row 8 in monkey J, row 6.5 in monkey Y). However, statistical analysis of the spatial distribution of SMA PStF effects failed to support a significant difference in the localization of distal and proximal muscles (K–S, $P > 0.05$) (Fig. 3). A large number of PStS effects were obtained from SMA and found to be intermingled with PStF effects (Figs. 2 and 3). No significant differences in the representations of PStF and PStS were found except for wrist and digit muscles in monkey J (K–S, $P < 0.05$).

Distal muscles were preferentially represented in SMA for both PStF and PStS effects (Table 2). The muscles most commonly facilitated in decreasing order were FDP, FDS, and ED 2,3, and the ones most commonly suppressed were ED 2,3, FDP, EDC, and ADE (Fig. 4*A*). The number of flexors and extensors recorded at each joint was different for each monkey. For accurate comparison, the distribution of PStEs in muscles at each joint and across joints was normalized to 6 muscles (Fig. 5*C* and *D*). After normalization, PStF was more common in flexors than extensors at the elbow ($P = 0.02$, Chi-Square test) and there was also a tendency toward flexor dominance among wrist and digit muscles. There were 39 (23.8%) sites from both animals where distal and proximal muscles were cofacilitated (Fig. 3).

The mean muscle field (number of muscles showing PStEs) from sites of stimulation within SMA, including both PStF and PStS effects, was 2.5 ± 2.0 (total of 208 sites). When considering sites where only PStF effects were present (107 sites throughout SMA), the mean muscle field size was 1.9 ± 1.8. Only 21 sites had 5 or more PStEs and the majority of these were located in the deepest, posterior part of SMA. At sites where more than one PStE was present (total), the majority of them showed a combination of PStF and PStS (56 sites, muscle

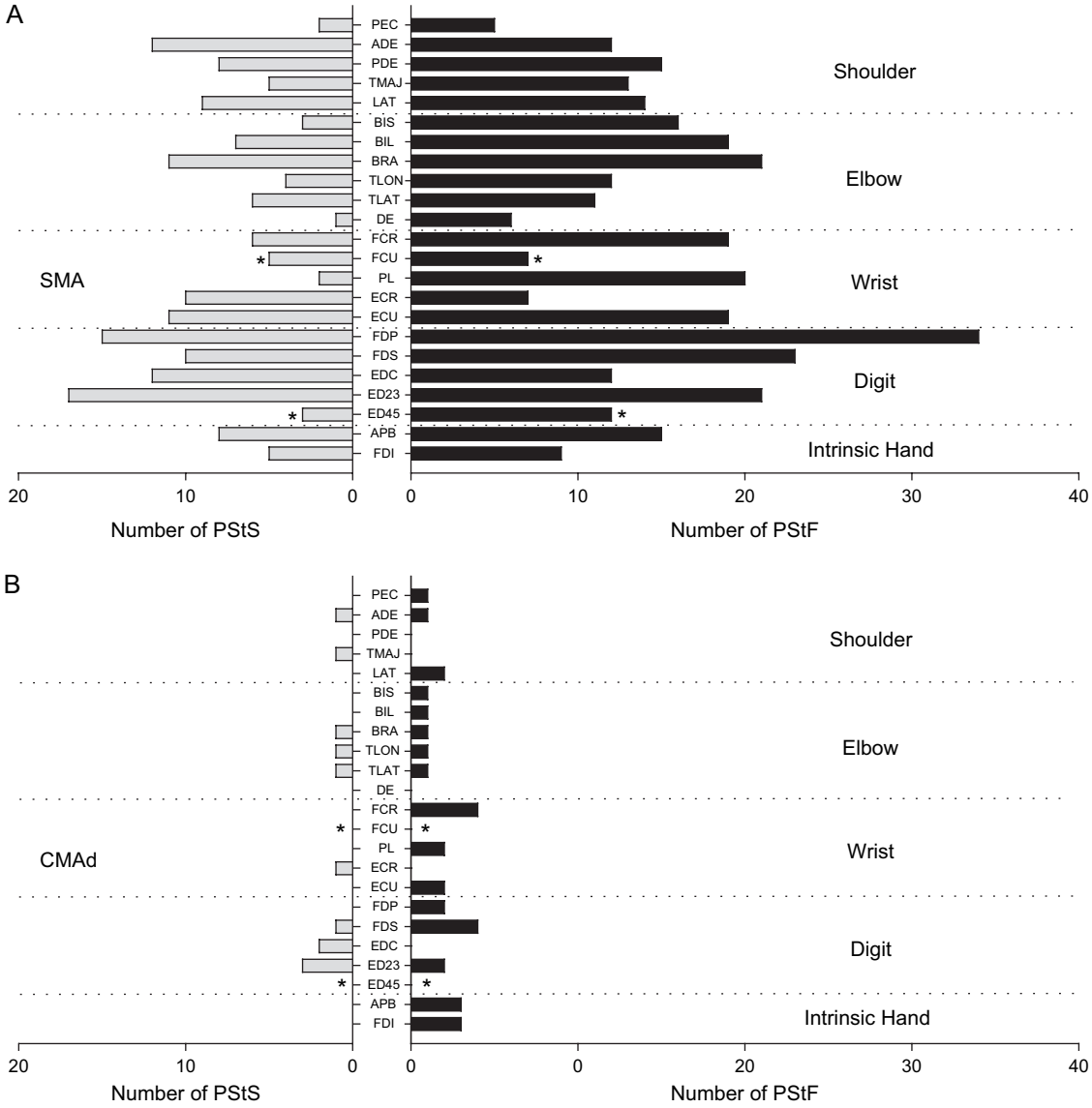

Figure 4. Distribution of PStF (right) and PStS (left) obtained from 19 to 23 muscles of the forelimb for SMA (*A*) and CMAd (*B*). The dotted lines separate muscles belonging to different joints. See Materials and Methods for muscle abbreviations. The asterisk (*) on muscles FCU and ED 4,5 indicates effects from monkey J only. Because of the combination of muscles formed to produce TRI and Intrins. in monkey Y, the total number of effects in these muscles was divided by 2 and distributed equally in muscles labeled TLON and TLAT and in muscles labeled FDI and APB.

field of 3.9 ± 2.1); fewer sites evoked only PStF (40 sites, muscle field 3.5 ± 2.1) or only PStS effects (20 sites, muscle field 3.0 ± 0.7 muscles).

Examples of PStEs from SMA and M1

Figure 6 shows typical PStEs at 60 μA from one site in SMA. This site was located in the posterior part of SMA. At this location, a large number of PStEs were produced in distal muscles. For comparison, effects from a site in M1 are shown at 15 and 60 μA. The SMA site produced facilitation in 9 of 12 distal muscles, including both flexors and extensors, and also showed a significant effect in the elbow muscle BRA. The M1 site produced PStF in both distal and proximal muscles at 15 μA and was selected because it yielded effects in many of the same muscles as the SMA site. PStEs from M1 at 15 μA were greater in magnitude compared with those from SMA at 60 μA. At 60 μA, the number of PStEs from M1 grew to include nearly all of the recorded muscles and the magnitude increased almost 10-fold in some muscles. The strongest effect from SMA at the site illustrated was 23 ppi in FDS and FCU. In contrast, the strongest effect at 60 μA from the M1 site was nearly 10 times greater (224 ppi in APB). PStF effects produced from M1 at 60 μA were significantly wider (mean ± SD; 10.0 ± 5.1 ms) than those from M1 at 15 μA (5.3 ± 2.7 ms) and those from SMA at 60 μA (5.7 ± 3.4 ms) ($P < 0.001$). The mean rise time (onset to peak) of PStF effects from M1 at 60 μA was also longer (3.7 ± 1.5) than effects at 15 μA (2.5 ± 1.5 ms) and effects from SMA at 60 μA (2.7 ± 2.4 ms) ($P < 0.001$).

Maps of CMAd Based on PStEs

Although data obtained for CMAd were more limited than for SMA, motor output maps constructed for CMAd suggest a tendency for proximal muscles to be located more posterior to distal muscles (monkey Y, Figs. 2 and 3). For PStF effects, as

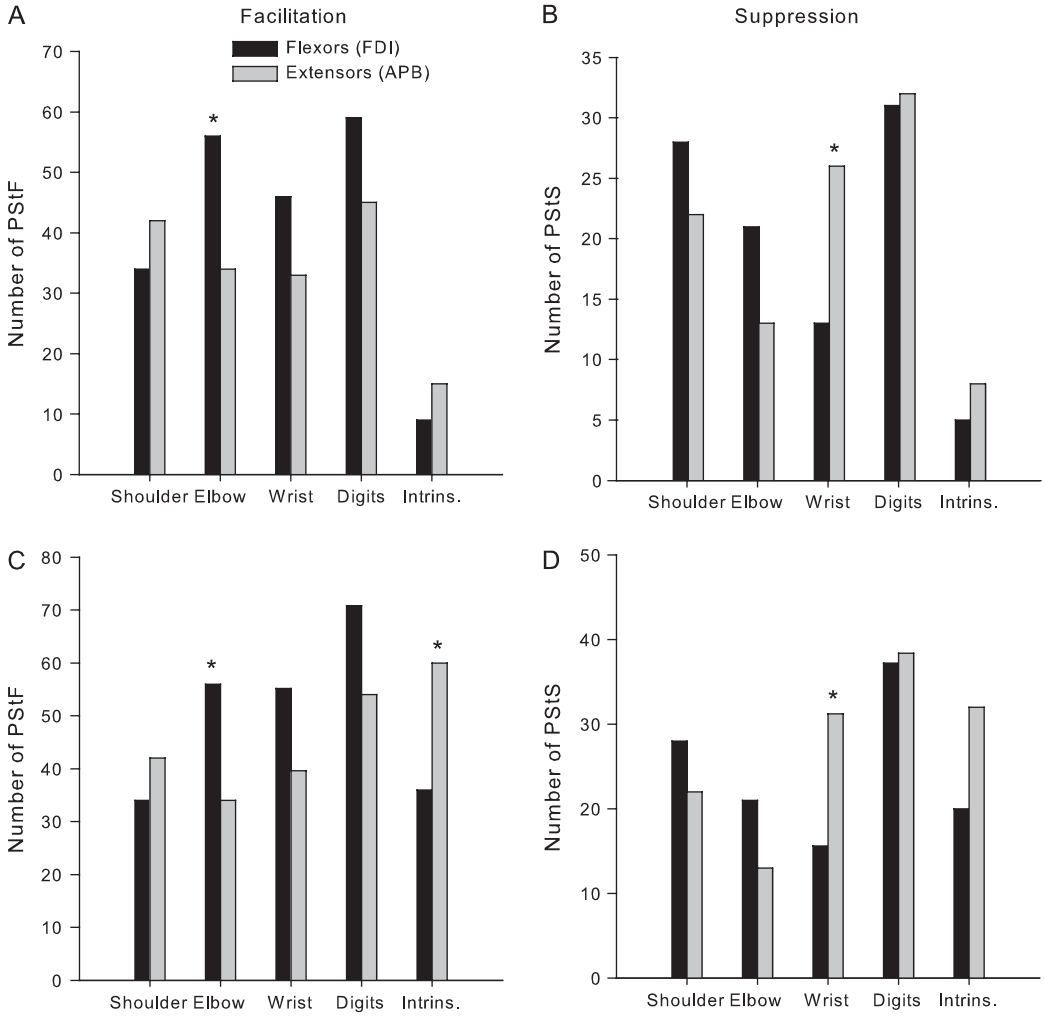

Figure 5. (*A*,*B*) Distribution of PStF and PStS from SMA in extensor and flexor muscles of the shoulder, elbow, wrist, and digits muscles after normalizing for differences in the number of flexor and extensor muscles recorded within each joint. Note that differences in the number of recorded muscles will influence the number of effects obtained. Flexor–extensor differences at each joint were normalized to the muscle group (flexor or extensor) with the greater number of recorded muscles. (*C*,*D*) Distribution of PStF and PStS from SMA after further normalizing the data in (*A*,*B*) for differences in the number of muscles recorded across joints. In this case, the number of effects at each joint were normalized to 6 muscles, which was the actual number recorded at the elbow joint. Intrinsic muscles FDI and APB are plotted as flexor and extensor respectively. Significant differences based on Chi-Square analysis at $P \leq 0.05$ level are indicated with an asterisk.

with SMA, distal muscles were preferentially represented, particularly the flexors FCR and FDS, and the intrinsic hand muscles APB and FDI (Table 2, Fig. 4*B*). PStS effects were also more common in distal muscles, particularly in ED 2,3 and EDC, antagonists of muscles showing the most PStF effects. In CMAd, PStF effects (excluding intrinsic hand muscles) were significantly more common in flexors (70%) than in extensors (30%) and the same was true of PStS effects (69% vs. 31%, respectively) ($P < 0.001$, Chi-Square test). The muscle field based on StTA of EMG activity including both PStF and PStS effects was 1.4 ± 0.7 and 1.3 ± 0.6 when considering only PStF effects. Only 2 sites had 3 PStEs (most observed) and only 1 site showed cofacilitation of flexors and extensors.

Distribution of PStF Latencies

The distributions of PStF onset latencies from SMA, CMAd, and M1 at 60 μA are given in Table 2 and Figure 7*A*. Compared with SMA and CMAd, the onset latencies of PStF from M1 were shorter and less broadly distributed. A very narrow unimodal distribution of PStF latencies was observed for effects from M1. PStF at 60 μA from M1 had average onset latency shorter by 8 and 12.1 ms compared with effects from SMA and CMAd, respectively (One way analysis of variance, $P < 0.001$). The PStF latencies from SMA were shorter than those from CMAd ($P < 0.001$).

Only 35 PStF effects from SMA (10% of all SMA PStF effects) had latencies less than or equal to the mean M1 latency. Among these, 54% came from distal muscles and 46% from proximal muscles. However, it is noteworthy that the shortest PStF latencies from SMA were as short (within 0.5 ms) as the shortest latency effects in the same muscles obtained from M1 at 60 μA. These effects were all in digit and intrinsic hand muscles. For CMAd, 7 PStF effects (21% of all CMAd PStF effects) had latencies less than or equal to the mean M1 latency, including 6 effects in distal muscles and 1 effect in a proximal muscle (LAT). The shortest PStF latency from CMAd (5.75 ms) was in LAT and was as short as the latency from M1.

Comparison of PStF Latencies at Different Joints

The average latencies of PStF from SMA and CMAd were longer than those from M1 at 60 μA in the corresponding joints ($P <$

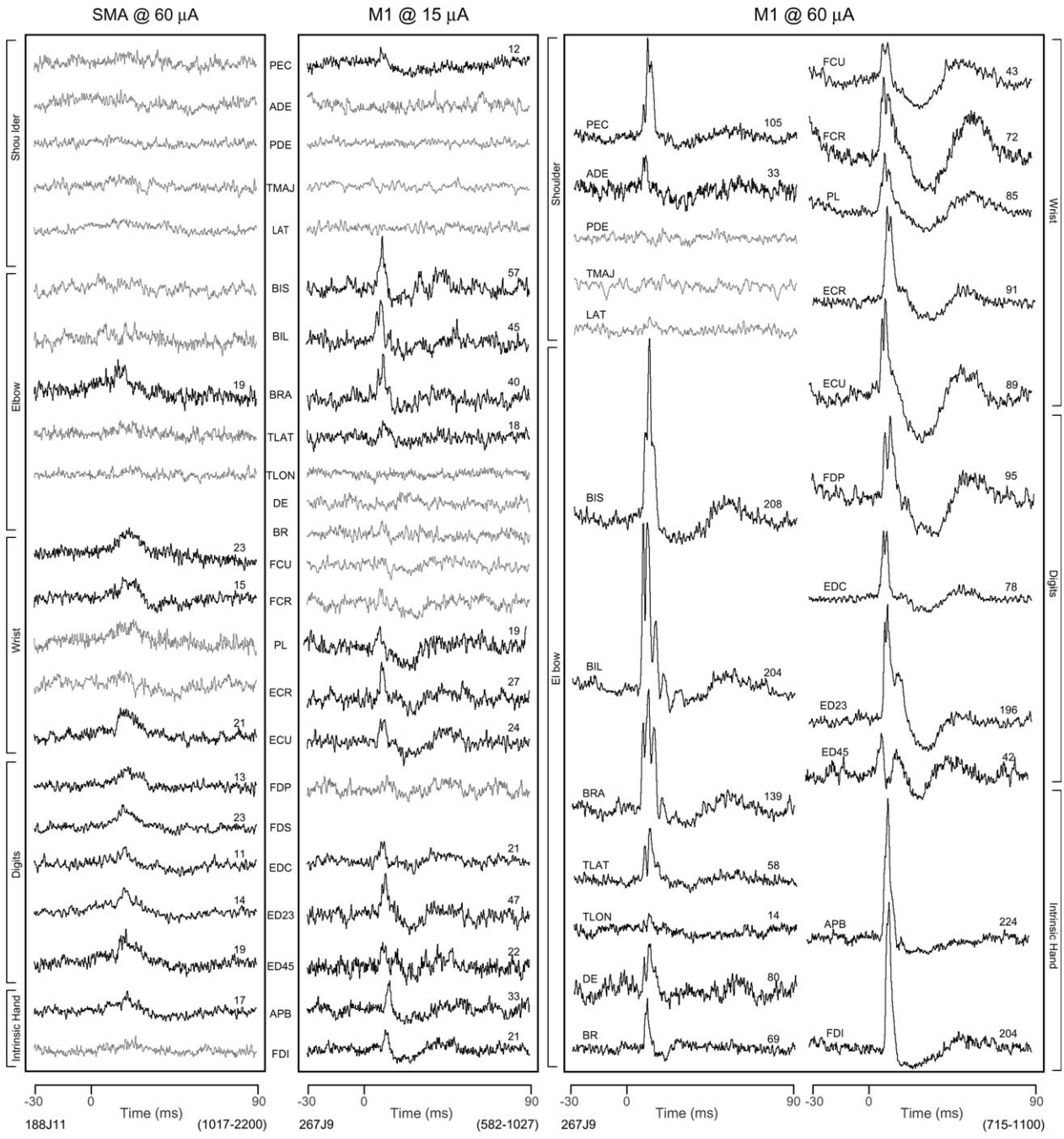

Figure 6. StTAs of forelimb muscles from 1 SMA site (188J11) at 60 μA and 1 M1 site (267J9) at 2 different intensities, 15 and 60 μA. Time zero corresponds to the stimulus used for constructing the average. PStF were observed in records shown in bold and no poststimulus effects in lighter gray. The range of number of trigger events for different muscles is given in parenthesis at bottom of each panel. The number above each record is the magnitude of the effect expressed as ppi over baseline.

0.001). Comparison of latencies in corresponding joints revealed longer latencies in CMAd compared with SMA for elbow, wrist, and digit muscles ($P < 0.001$). Comparison of the latencies between joints obtained for the same motor area did not reveal significant differences for either SMA or CMAd ($P > 0.05$) despite a clear trend toward shorter PStF latencies for effects in both the most proximal and the most distal joints from SMA and a trend toward shorter latencies for effects in the most distal muscles from CMAd (Fig. 8*A*). Only M1 PStF effects showed significantly shorter latencies in proximal muscles compared with those from distal muscles ($P < 0.001$) (Table 2). Increasing stimulus intensity from 15 to 60 μA in M1 resulted in a significant shortening of PStF latency by an average of 1.1 ms ($P < 0.001$).

Distribution of PStF Magnitudes

The distribution of magnitudes expressed as ppi shows vastly stronger effects from M1 compared with SMA or CMAd ($P < 0.001$) (Fig. 7*B*). The magnitudes of the effects from M1 were on average ~10-fold stronger than those from SMA or CMAd (Table 2). This magnitude difference is somewhat less than the 15-fold difference previously estimated based on extrapolated 60-μA

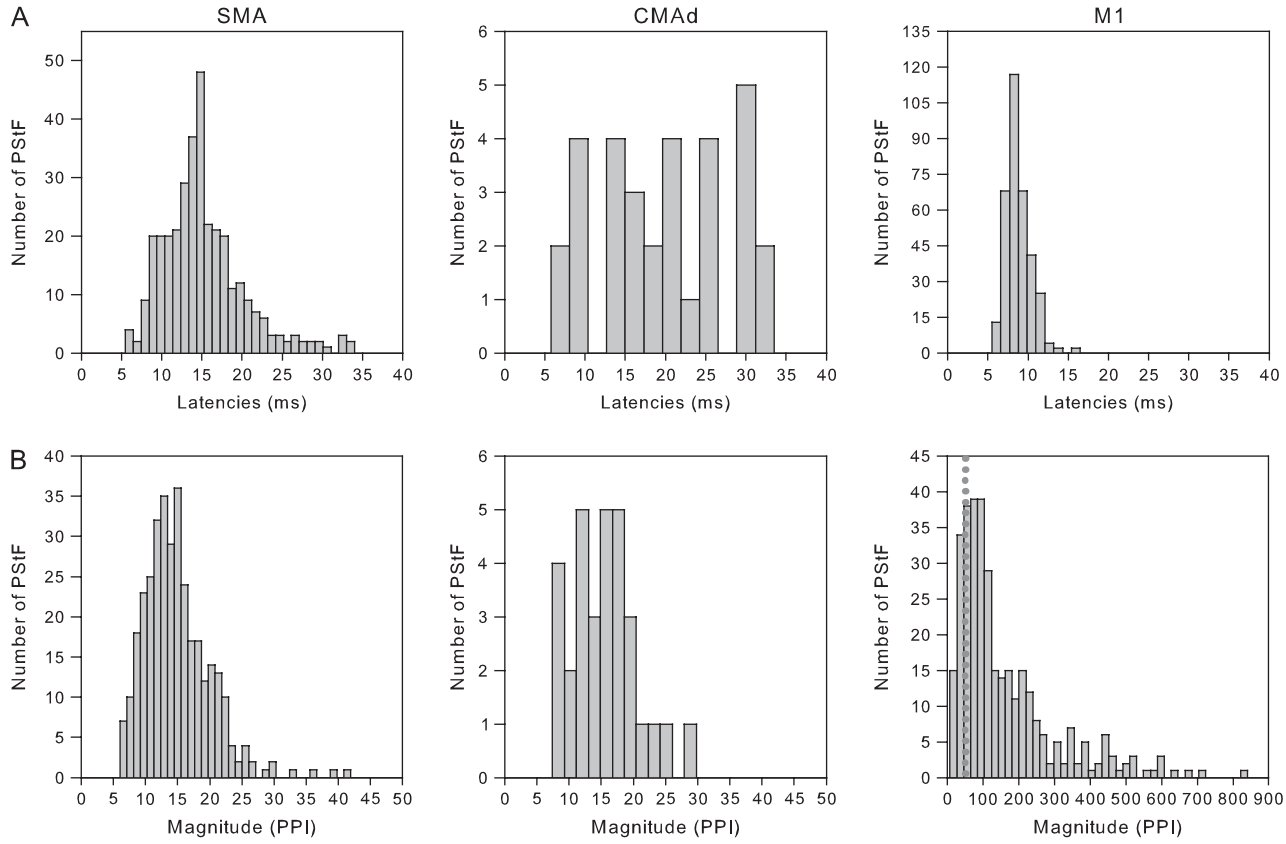

Figure 7. (*A*) Distribution of PStF onset latencies for SMA, CMAd and M1 at 60 μA for muscles at all forelimb joints ($N = 341$ for SMA, $N = 33$ for CMAd, and $N = 340$ for M1). (*B*) Distribution of PStF magnitudes at 60 μA for SMA, CMAd, and M1 for muscles at all forelimb joints. Note that the plots have different magnitude scales. The magnitudes are expressed as a ppi over baseline. The doted line in the graph of magnitudes for M1 corresponds to the highest magnitude effect in the SMA and CMAd histograms.

magnitudes of PStEs in M1 (Boudrias et al. 2006). However, the magnitude of M1 effects in distal muscles was ~13-fold greater than CMAd or SMA. Increasing stimulus intensity from 15 to 60 μA produced a proportional increase in PStF magnitude in distal and proximal muscles of ~4-fold (Table 2). The PStF magnitudes from CMAd were not different than those from SMA ($P > 0.05$). In SMA, 51 effects had magnitudes above 20 ppi (15% of all effects), 3 effects had magnitudes above 30 ppi (PL, ppi = 33; TMAJ, ppi = 36; ADE, ppi = 39), and 1 proximal muscle had PStF with a magnitude above 40 ppi (TMAJ, ppi = 42). CMAd had 5 PStF effects (16% of all PStF) with magnitudes above 20 ppi, all originating from distal joints.

Comparison of PStF Magnitudes at Different Joints

The average magnitudes of PStF from SMA and CMAd were all weaker than the effects from M1 at 60 μA in the corresponding joints ($P < 0.001$) (Fig. 8*C*). There was no difference in the magnitudes of effects in the corresponding joints between SMA and CMAd, nor was there a difference in the magnitude of effects across joints for SMA or CMAd ($P > 0.05$). Distal muscles showed the strongest PStF magnitudes from CMAd and M1 ($P < 0.04$, $P < 0.001$, respectively). No difference was found between the magnitudes of effects at distal and proximal joints for SMA ($P > 0.05$) (Table 2). We observed the same progressive trend of increased magnitude of M1 PStF from proximal to distal muscle groups at an intensity 60 μA as previously reported for 15 μA (Park et al. 2004). This consistent increase in magnitude was not observed for SMA or CMAd (Fig. 8*C*).

Distribution of the Onset Latencies and Magnitudes of PStS

PStS onset latencies from SMA and CMAd were substantially longer ($P < 0.001$) than those from M1 at 60 μA (Table 2 and Fig. 8*B*). PStS latencies from CMAd and SMA were not different from each other ($P > 0.05$). The mean onset latency of PStS in distal compared with proximal muscles was not different for effects from M1, SMA, or CMAd ($P > 0.05$). Whereas M1 PStF latencies became shorter at higher intensities of stimulation, shortening of latency was not observed for PStS ($P > 0.05$) (Fig. 8*B*). It should be emphasized that our data set for this issue is based on a relatively small number of effects because most of the pure PStS effects gained an earlier PStF when stimulation was applied at 60 μA. Of 52 pure PStS effects obtained from M1 sites at 15 μA, only 11 remained uncontaminated by an earlier PStF at 60 μA. The sample size of PStS effects from CMAd was also relatively small. This may explain the irregular shape of the latency plot for CMAd in Figure 8*B* including the larger standard error of mean (SEM) and the absence of PStEs for intrinsic hand muscles.

The average magnitudes of PStS from SMA and CMAd were half as large as the PStS from M1 at 60 μA ($P < 0.001$). Because most pure PStS effects were contaminated by facilitation at 60 μA, –28.6 ppi may be a significant underestimate of the strength of suppression from M1. PStS magnitudes from CMAd and SMA were not different from each other ($P > 0.05$). Magnitudes of PStS effects at proximal versus distal joints also were not different when compared within the same motor area ($P > 0.05$).

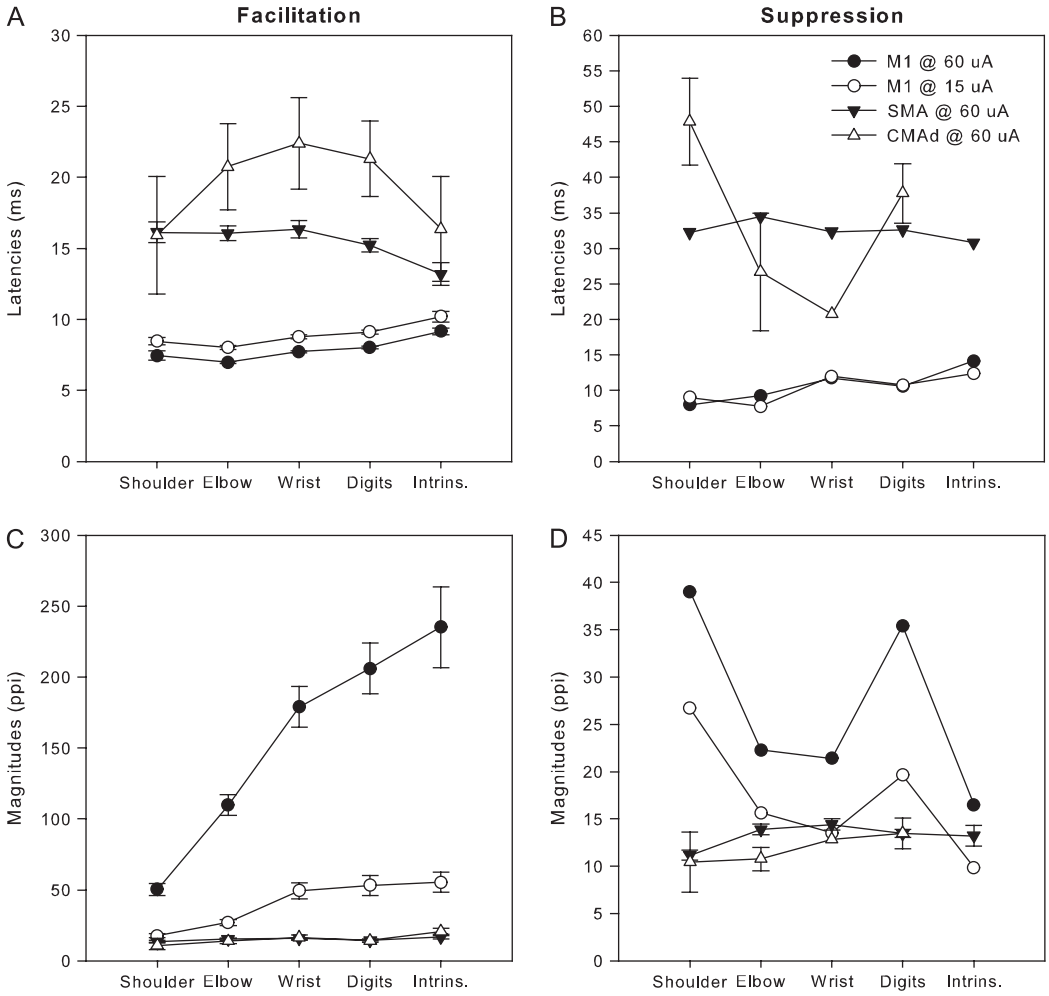

Figure 8. Comparison of the onset latencies and magnitudes of PStEs from SMA, CMAd, and M1 at different joints (shoulder, elbow, wrist, digit, and intrinsic hand muscles). Two different stimulation intensities were used for M1 (15 and 60 μA). (*A*,*B*) Summed latencies of facilitation and inhibition of PStEs at each joint in 2 monkeys. For facilitation effects, $N = 341$ for SMA, $N = 31$ for CMAd, $N = 350$ for M1 at 15 and 60 μA. For suppression effects, $N = 172$ for SMA, $N = 12$ for CMAd, $N = 11$ for M1 at 15 and 60 μA. (*C*,*D*) Summed magnitudes of facilitation and suppression of PStEs at each joint of 2 monkeys. No PStS were present in CMAd for intrinsic hand muscles. The bars represent the SEM.

The strongest PStS effect from M1 was in ED 2,3 (ppd = –65). SMA produced the greatest number of PStS effects, with the majority occurring in distal muscles (Table 2). The muscles with the largest number of PStS effects were ED 2,3, FDP and EDC for SMA, and ED 2,3 and EDC for CMAd (Fig. 4*B*). Across joints, SMA PStS effects were weaker in shoulder muscles than elbow, wrist, and intrinsic hand muscles ($P < 0.002$). The strongest PStS effects from SMA, in decreasing order, were in ECU, FCU, EDC, and BRA with magnitudes between –22 and –27 ppd.

PStEs from the Ipsilateral SMA

It is known that a large percentage (23%) of SMA terminations are on the ipsilateral side in the cervical enlargement of the spinal cord (Dum and Strick 1996). To investigate the efficacy of these connections, a total of 13 tracks were performed in SMA ipsilateral to the recorded muscles of both monkeys. Nine PStEs were obtained from ipsilateral SMA, including 7 PStF and 2 PStS effects. These effects had average latencies of 10.1 ± 3.3 and 19.0 ± 3.2 ms, and magnitudes of 13.5 ± 4.1 ppi and –12.6 ± 1.1 ppd for PStF and PStS, respectively. Although the sample size is small, latencies from the ipsilateral SMA were shorter than those observed for the contralateral SMA ($P < 0.004$). The magnitudes were similar to the means of effects from contralateral SMA ($P > 0.05$). The majority of PStF effects were in distal muscles ($N = 6$). The shortest latency and the strongest magnitude effects observed from the ipsilateral SMA were in ECU and ADE, respectively. The 2 PStS effects were in distal muscles.

Discussion

We wish to emphasize 4 major findings from the present study. First, our data based on StTAing of EMG activity suggest that the distal and proximal forelimb muscles representations in SMA are not segregated as reported previously for M1 (Park et al. 2001). Second, using the same parameters of stimulation, the magnitudes of PStF effects on forelimb muscles from SMA and CMAd are on average one-tenth those from M1. Third, although our sample of PStEs from CMAd is relatively small, the effects obtained resemble those from SMA in terms of latency and magnitude. Finally, a small number of PStF effects from SMA and CMAd had onset latencies as short as the shortest M1 latencies suggesting that at least some of the corticospinal neurons in these areas have linkages with motoneurons that are as direct as those from M1.

Forelimb Organization of SMA

Proximal and distal forelimb representations were not found to be clearly segregated in SMA, although a tendency toward separation was present (see below). A large majority of stimulated sites facilitated only proximal or distal muscles: Only 23.8% sites, mainly located on the mesial wall, cofacilitated both proximal and distal muscles. This contrasts with the M1 forelimb representation, which is organized into a segregated core of distal muscle representation surrounded by a horseshoe-shaped proximal muscle representation (Park et al. 2001). The proximal and distal representations were separated by a large zone producing effects in both proximal and distal muscles. This zone was termed the proximal–distal cofacilitation zone and was viewed as well suited to produce the patterns of distal and proximal muscle coactivation needed for coordinated multi-joint movements. The maps for M1 were based on data obtained at 15 μA raising the question of what the maps would look like if they had been done at 60 μA and specifically if there would still be clearly separable distal only, proximal only and distal–proximal zones. Unfortunately, we do not have a complete map of M1 based on 60 μA data. Nevertheless, it is possible to use the 15 μA data and knowledge of current spread to model what the 60 map would look like. The model was based on estimating physical current spread from the expression $r =$, where r is the radius of activated tissue, i is the current intensity, and k is the excitability constant. There are a wide range of estimates for the excitability constant (Cheney and Fetz 1985; Tehovnik et al. 2006) although a constant of about 300 $\mu A/mm^2$ would certainly be considered minimal. A minimal k value will produce the greatest expansion of excitatory current spread and will yield conditions least favorable for retaining separable distal only and proximal only representations. Nevertheless, in applying this model of physical current spread to the actual map obtained at 15 μA for 2 monkeys, we still found clearly separable distal only and proximal only output zones. Therefore, we believe the differences in separation of distal and proximal representations in SMA compared with M1 are real and not a consequence of using different stimulus intensities.

The lack of topographic organization within the forelimb representation of SMA has been noted in a number of studies in which ICMS was used to evoke movements (Macpherson J et al. 1982; Mitz and Wise 1987; Luppino et al. 1991). An imprecise topographic organization of neurons projecting from SMA to the distal and proximal parts of forelimb M1 was also observed in the retrograde labeling study of Tokuno and Tanji (1993). Distal and proximal neurons were found to be largely intermingled within SMA and only a few double-labeled neurons were observed. The lack of segregation of SMA's forelimb representation may contribute to the integration of signals needed for coactivation of distal and proximal muscles during execution of coordinated multi-joint movements.

These results appear to differ from those of He et al. (1995) who reported that areas of SMA projecting most densely to the upper and lower cervical segments of the spinal cord (proximal and distal muscles respectively) were largely separate. This was based on analysis of the most densely labeled 200-μm bins (high density bins) of corticospinal neurons following tracer injections into the upper and lower segments of the cervical spinal cord. However, as He et al. (1995) also point out, the spatial distributions in SMA of individual corticospinal neurons labeled from upper versus lower cervical cord injections were highly overlapping. Our findings are certainly consistent with this result, but there is also a suggestion in our data of the separation of proximal and distal representations noted by He et al. (1995) based on high-density bin analysis. Although differences in the spatial distributions of distal and proximal sites in our data were not statistically significant, careful inspection of Figure 3 shows a tendency for proximal muscle sites to be located more anteriorly and laterally than distal muscles sites (particularly in monkey J), which is similar to the distribution of corticospinal neurons labeled from upper cervical spinal cord injections (yellow dots in Fig. 10 of He et al. 1995). Spread of effective current associated with ICMS techniques seems unlikely to be a source of differences between our results and those from anatomical studies based on injections of retrograde tracers. For example, we estimate that a 60-μA stimulus would have activated corticospinal neurons within a 210-μm radius (Stoney et al. 1968; Ranck 1975; Tehovnik 1996; Park et al. 2001). This is not sufficient to explain the separation of labeling associated with upper versus lower cervical cord injections reported by He et al. (1995). Of course, in addition to direct physical spread of stimulating current, an unknown amount of physiological spread could have occurred, although this would have been greatly minimized by the low stimulus frequencies of StTAing.

Some ICMS studies have shown that distal forelimb movements were evoked from sites located in the deepest posterior part of the mesial aspect of SMA (Macpherson JM et al. 1982; Luppino et al. 1991). This region corresponds to the distal representation of corticospinal neurons based on injections of retrograde tracers into the lower cervical segments of the spinal cord. We also found an area where a large number of PStEs were produced in distal muscles (Fig. 3), consistent with He et al. (1995), but this aspect of spatial segregation failed to achieve statistical significance. In contrast to studies based on ICMS-evoked movements showing that proximal muscles of the forelimb were either preferentially represented in SMA (Luppino et al. 1991) or equally represented with distal muscles (Mitz and Wise 1987; Inase et al. 1996), a majority of our PStF effects were in distal muscles. One factor that might have contributed to this discrepancy is that at many posterior sites in the deepest part of SMA, the number of distal muscles with effects exceeded the average muscle field size. For example, the cortical site represented in Figure 6 was in the deepest posterior portion of SMA and had PStEs in 10 muscles, 9 of which were distal muscles. Our conclusion is based, in part, on the total number of distal versus proximal muscles with effects whereas previous studies did not quantify effects at the level of individual muscles.

Forelimb Organization of CMAd

Only a few studies have used ICMS to assess the distribution of evoked movements in CMAd (Luppino et al. 1991; Akazawa et al. 2000; Takada et al. 2001; Akkal et al. 2002). The majority of these studies have reported a segregated forelimb representation located rostrally to a smaller hindlimb representation. Based on injections of retrograde tracers in upper and lower segments of the cervical spinal cord, the forelimb representation of CMAd was reported to contain 4 times as many corticospinal neurons associated with distal muscles than proximal muscles (He et al. 1995). Although our data set consists of a relatively small number of PStEs from CMAd derived largely from one animal, our results do confirm that

forelimb muscles are represented in CMAd and that PStEs are largely distributed to distal muscles.

We found a representation of distal muscles that extended rostro-caudally over CMAd and a proximal representation located dorsally to the distal one and somewhat caudal. This is in general agreement with the forelimb organization based on the anatomical studies of He et al. (1995). In their study, distal corticospinal neurons formed 2 islands within CMAd's arm representation, a large one located rostrally and a smaller one located more caudally. Neurons involved in the control of proximal muscles were located dorsally within the larger distal arm representation of CMAd. We were unable to adequately determine if a second segregated representation of distal muscles exists in the caudal part of CMAd because we did not perform tracks that far caudally.

Latency and Magnitude of PStF Effects from SMA, CMAd, and M1

A few PStF effects from SMA and CMAd had onset latencies as short as the shortest ones from M1. This suggests that at least a small fraction of corticospinal neurons in these areas are fast conducting and have linkages with motoneurons that are as direct as those from M1 (Maier et al. 2002). All of these effects from SMA were in distal muscles. This agrees with anatomical studies demonstrating terminations from SMA and CMAd in the ventral horn of the spinal cord (Dum and Strick 1996; Rouiller et al. 1996) and with intracellular evidence supporting monosynaptic connections (Maier et al. 2002). However, at 60 μA, the latencies of PStF effects from SMA and CMAd were, on average, 8–12 ms longer than those from M1 suggesting that the predominant linkage to motoneurons is less direct. This more indirect linkage is consistent with the fact that corticospinal terminations from SMA and CMAd are concentrated in the intermediate zone of the spinal cord (laminae V–VIII) where various populations of interneurons are located (Dum and Strick 1996). However, it should be noted that the dendrites of spinal motoneurons do project into the intermediate zone, so observing that the terminations of corticospinal neurons are restricted to the intermediate zone would not rule out the presence of direct synaptic connections with motoneurons (Porter and Lemon 1993). Longer latencies from SMA and CMAd are also consistent with the smaller size of their neurons compared with M1 (Dum and Strick 1991).

Effects from SMA and CMAd were substantially weaker in magnitude compared with those from M1. This result stands in contrast to the fact that the density of corticospinal neurons in SMA and CMAd is very similar to that of M1 (Dum and Strick 1991). Given the relatively limited spread of effective current from even a 60-μA stimulus, we would argue that corticospinal cell density is the parameter that should reflect the magnitude of output effects rather than the total number of corticospinal neurons a motor area contains (He et al. 1995). Accordingly, we conclude that corticospinal neurons arising from SMA and CMAd are organized in a very different way in terms of spinal connectivity and probably with fundamentally different functions than M1 corticospinal neurons. As suggested previously, the major contribution of SMA and CMAd to movement initiation and control might be achieved through cortico-cortical connections with M1 and/or innervation of spinal interneurons influencing reflex and other spinal circuits rather than providing direct input to motoneurons (Boudrias et al. 2006).

Stimulation restricted to layer V of the cortical gray matter of SMA did not significantly alter the latencies of PStF and PStS effects compared with our previous study based on effects collected from all cortical layers of SMA ($P > 0.05$) (Boudrias et al. 2006). However, the magnitudes of PStF and PStS effects for sites in or near layer V from this study were stronger than those based on all cortical layers ($P < 0.007$). This is consistent with more effective activation of corticospinal neurons when stimulation is applied directly to layer V.

Potential Effect of Cell Size on Observed Strength of Output Effects

It is an accepted principle that the smaller the axon, the greater will be the extracellular stimulus current required for its activation. The possibility that this principle might also apply to the electrical excitability of cortical neurons raises the issue of how this might have affected our results. To evaluate this issue, the first question that needs to be addressed is whether corticospinal neurons in SMA actually do differ significantly in size from those in M1 and, if they do, by how much. Dum and Strick (1991) have provided detailed measurements of the soma diameters of corticospinal neurons in the arm representation of M1 and premotor areas including SMA. In M1, the soma sizes range from 9 to 31 μm with a mean of 17.5 μm compared with a range of 8–32 μm with a mean of 14.5 μm for SMA. Clearly, the average corticospinal cell in M1 is somewhat larger than SMA but to what extent could this have contributed to our finding of weaker output effects from SMA with StTAing? The answer to this question requires knowing the relationship between neuronal size and threshold for electrical stimulation. Is there a direct relation as there is for axons in peripheral nerves? Stimulation of gray matter with a microelectrode is a more complex set of conditions and specific studies of excitability in relation to cell size are more limited and difficult to interpret. The relationship between threshold current and distance from a neuron is given by $i = kr^2$ where i is the stimulus current, r is the distance from the electrode to the cell and k is the excitability constant (Tehovnik et al. 2006). In a study of cortical pyramidal tract neurons, Stoney et al. (1968) reported that the excitability constant k was inversely correlated with antidromic latency. However, the authors did not give the actual antidromic latencies of the cells they tested, so it is difficult to infer from their data the magnitude of the relationship between cell size and excitability. Nevertheless, because antidromic latency is directly related to conduction velocity and conduction velocity, in turn, is directly related to soma size (Sakai and Woody 1988), this result suggests that large pyramidal tract neurons might be activated at lower stimulus currents than smaller pyramidal neurons at the same distance from the stimulating electrode. However, in contrast, rigorous modeling of extracellular neuronal stimulation actually suggests that the opposite relationship might apply, namely, that larger neurons should have higher thresholds for extracellular electrical stimulation (Rattay 1999). It should also be noted that the relationship between k and conduction velocity reported by Stoney et al. (1968) applies to direct activation of pyramidal tract neurons, not synaptic activation. Evidence currently available supports the view that ICMS activates corticospinal neurons through a mechanism that is predominately transynaptic rather than direct (Jankowska et al. 1975). To conclude, it is possible that differences in corticospinal cell size between M1 and SMA could have had some

effect on our results, but it seems highly unlikely, given the evidence discussed above, that differences in excitability stemming from an average difference in cell size of 18% would have contributed much to the 10-fold difference in strength of output we have observed between SMA and M1.

General Comparison of SMA, CMAd, and M1 Output Properties

In line with the unique role of M1 in forelimb motor control, many differences in the nature of the output properties from SMA and CMAd were observed in comparison to Park et al. (2004) based on complete mapping of M1 using StTAs of EMG activities at 15 μA. The progressive increase in magnitude of PStF going from the most proximal to the most distal muscles, which was clear for M1, was absent for SMA and CMAd. There was less divergence of output effects to multiple muscles as the muscle field based on StTA of PStEs was smaller for SMA and CMAd compared with M1. The average muscle-field size (PStF only) for M1 at 60 μA was 12.6 compared with 6.2 muscles at 15 μA (Park et al. 2001). The comparable number for SMA at 60 μA was 2.6 (PStF only). It should be noted that our M1 data at 60 μA were not based on a systematic sampling of the entire M1 representation although it does include both deep and surface M1 sites. Nevertheless, it is clear, that sites in M1 activate a much larger number of muscles than sites in SMA. This implies that the output from SMA targets a more restricted set of muscles than the output from M1. However, an alternative explanation might be that because the effects from SMA are weaker than M1, synaptic linkages to some muscles are escaping detection. In an effort to minimize this possibility, we set the minimum number of acceptable trigger events for SMA at double that for M1 (1000 vs. 500). Also, for proximal muscles, the average magnitude of PStF from M1 at 15 μA was similar to that from SMA at 60 μA (24 vs. 15 ppi) and yet the muscle-field size for proximal muscles only was still much smaller for SMA compared with M1 (1.5 vs. 6.3). Therefore, we conclude that there is a real difference in muscle-field size reflecting underlying synaptic connections. We would suggest that under normal conditions, M1 corticospinal neurons exert a dominant role in establishing synaptic linkages with motoneurons and block or crowd out SMA corticospinal connections. Of course, with damage to M1, this balance might change.

Finally, a greater proportion of sites in M1 (42%) showed cofacilitation of flexors and extensors compared with SMA and CMAd. Whereas extensors were more commonly facilitated and flexors suppressed from M1, the opposite was true of SMA. However, common features including preferential activation of distal muscles and comparable proportions of PStF and PStS were shared among SMA, CMAd, and M1.

Output effects from CMAd were very similar to those from SMA. With few exceptions, no differences were observed between the latencies and the magnitudes of their PStEs. This suggests that CMAd parallels SMA in terms of its capacity to influence muscle activity and movement. Single unit recordings have also reported remarkable similarities between CMAd and SMA in the roles they may play in the production of visually guided arm movements (Russo et al. 2002).

In a previous paper, we compared the output properties of SMA at 60 μA with extrapolated values of PStEs from M1 based on measured M1 PStEs obtained at an intensity of 15 μA (Park et al. 2004; Boudrias et al. 2006). In the current study, the selection of the M1 data set required PStEs in the same muscles at an intensity of 15 and 60 μA. The latency of PStF effects at 60 μA was on average 1.1 ms shorter than at 15 μA. This is consistent with the reduced utilization time at 60 μA as well as the likely greater involvement of direct rather than synaptic activation of corticospinal neurons (Cheney and Fetz 1985). At 60 μA, the magnitude of PStF effects quadrupled; peaks became wider and rise times longer (Fig. 6). This can be explained, at least partially, by greater physical and physiological spread of effective stimulus current at 60 μA compared with 15 μA (Jankowska et al. 1975; Park et al. 2001). Widening of effects at higher stimulus intensities might result from dispersion of latencies associated with recruitment of corticospinal and motoneurons with different conduction velocities, recruitment of less direct synaptic pathways, and recruitment of motor units with longer duration action potentials.

Distribution of Suppression Effects in SMA, CMAd, and M1

The latency of PStS from M1 was ~3 ms longer than the latency of PStF reflecting a less direct coupling, for example, the presence of an additional synapse, possibly a spinal inhibitory neuron, interposed between the corticospinal neurons and the motoneurons (Kasser and Cheney 1985). The latencies of PStS from SMA and CMAd were longer and the distribution broader than PStS from M1. This difference in latency of PStS is difficult to attribute entirely to a cortico-cortical mechanism involving M1. For example, inhibition of M1 pyramidal tract neurons by stimulation of SMA has a mean onset latency of only 6.7 ms (Tokuno and Nambu 2000), far less than the observed difference of 22–24 ms in the present study. Neither is the latency difference consistent with excitation of M1 neurons producing interneuronally mediated inhibition of motoneurons. The large number of PStS effects produced in distal and proximal muscles from SMA may be important for planning the temporal organization of movements, as reported in single unit recording studies (Mushiake et al. 1991; Tanji and Shima 1994; Clower and Alexander 1998; Shima and Tanji 1998).

The majority of M1 PStS effects obtained at 15 μA changed sign to become facilitatory at 60 μA so the number of effects that were present at both intensities was rather limited. Nevertheless, increasing the intensity of stimulation from 15 to 60 μA produced only a 1.5-fold increase in the magnitude of PStS. In fact, the magnitudes of PStS effects at intensities of 15 and 60 μA were not statistically different from each other ($P > 0.05$). In addition, the magnitudes of PStS effects did not follow the large increase observed for facilitation effects in going from proximal to distal muscles and did not show a preferential inhibition of the hand muscles. Moreover, latencies of PStS effects from M1 did not become significantly shorter at higher current intensities as observed for PStF effects from M1. One interpretation of these results is that inhibition reaches a maximum at the spinal level at relatively low intensities of stimulation. However, an alternative explanation is that our estimate of the growth in magnitude of inhibition with stimulus intensity is too low because the true level of suppression is being masked by much more powerful facilitation that occurs at 60 μA. In any case, weaker magnitude of PStS effects from SMA and CMAd compared with M1, as with the PStF effects, suggests a less effective coupling with inhibitory interneurons compared with M1.

Summary and Conclusion

Despite the fact that we quadrupled the number of tracks performed in SMA from our previous study (Boudrias et al. 2006), the resulting motor output maps for SMA did not reveal clearly segregated representations of proximal and distal forelimb muscles comparable with the segregated representations in M1. As for M1, we found that distal muscles are preferentially represented in SMA and CMAd. The presence of short onset latencies of PStF effects from SMA and CMAd suggest that at least some of their corticospinal neurons have synaptic linkages to motoneurons that are as direct as M1 corticospinal neurons. However, PStF effects from SMA and CMAd had latencies averaging 8–12 ms longer and magnitudes 9–10 fold weaker than those observed for M1. Our results demonstrate that the typical corticospinal neuron in SMA and CMAd provides relatively weak direct input to spinal motoneurons compared with the robust synaptic effects from M1. This suggests that the primary mechanisms by which SMA and CMAd influence motoneurons is predominantly indirect through innervation of interneurons in the intermediate zone of the spinal cord and projections to M1.

Funding

NIH grants NS39023, NS051825, P20 RR016475, NIH center grant HD02528, and a doctoral scholarship from "Les Fonds de la Recherche en Santé du Québec" (FRSQ-6389).

Notes

Conflict of Interest: None declared.

Department of Molecular and Integrative Physiology, University of Kansas Medical Center (KUMC), Kansas City, KS 66160-7336, USA Address correspondence to email: pcheney@kumc.edu

References

Akazawa T, Tokuno H, Nambu A, Hamada I, Ito Y, Ikeuchi Y, Imanishi M, Hasegawa N, Hatanaka N, Takada M. 2000. A cortical motor region that represents the cutaneous back muscles in the macaque monkey. Neurosci Lett. 282:125–128.

Akkal D, Bioulac B, Audin J, Burbaud P. 2002. Comparison of neuronal activity in the rostral supplementary and cingulate motor areas during a task with cognitive and motor demands. Eur J Neurosci. 15:887–904.

Asanuma H, Rosen I. 1972. Topographical organization of cortical efferent zones projecting to distal forelimb muscles in the monkey. Exp Brain Res. 14:243–256.

Belhaj-Saif A, Karrer JH, Cheney PD. 1998. Distribution and characteristics of poststimulus effects in proximal and distal forelimb muscles from red nucleus in the monkey. J Neurophysiol. 79:1777–1789.

Boudrias MH, Belhaj-Saif A, Park MC, Cheney PD. 2006. Contrasting properties of motor output from the supplementary motor area and primary motor cortex in rhesus macaques. Cereb Cortex. 16:632–638.

Cheney PD, Fetz EE. 1985. Comparable patterns of muscle facilitation evoked by individual corticomotoneuronal (CM) cells and by single intracortical microstimuli in primates: evidence for functional groups of CM cells. J Neurophysiol. 53:786–804.

Clower WT, Alexander GE. 1998. Movement sequence-related activity reflecting numerical order of components in supplementary and presupplementary motor areas. J Neurophysiol. 80:1562–1566.

Dum RP, Strick PL. 1991. The origin of corticospinal projections from the premotor areas in the frontal lobe. J Neurosci. 11:667–689.

Dum RP, Strick PL. 1996. Spinal cord terminations of the medial wall motor areas in macaque monkeys. J Neurosci. 16:6513–6525.

Galea MP, Darian-Smith I. 1994. Multiple corticospinal neuron populations in the macaque monkey are specified by their unique cortical origins, spinal terminations, and connections. Cereb Cortex. 4:166–194.

He SQ, Dum RP, Strick PL. 1995. Topographic organization of corticospinal projections from the frontal lobe: motor areas on the medial surface of the hemisphere. J Neurosci. 15:3284–3306.

Inase M, Sakai ST, Tanji J. 1996. Overlapping corticostriatal projections from the supplementary motor area and the primary motor cortex in the macaque monkey: an anterograde double labeling study. J Comp Neurol. 373:283–296.

Jankowska E, Padel Y, Tanaka R. 1975. The mode of activation of pyramidal tract cells by intracortical stimuli. J Physiol. 249:617–636.

Kasser RJ, Cheney PD. 1985. Characteristics of corticomotoneuronal postspike facilitation and reciprocal suppression of EMG activity in the monkey. J Neurophysiol. 53:959–978.

Kuypers HGJM. 1981. Anatomy of the descending pathways. In: Brookhart J, Mountcastle V, editors. Handbook of physiology—the nervous system II. Bethesda (MD): American Physiology Society. p. 597–666.

Luppino G, Matelli M, Camarda RM, Gallese V, Rizzolatti G. 1991. Multiple representations of body movements in mesial area 6 and the adjacent cingulate cortex: an intracortical microstimulation study in the macaque monkey. J Comp Neurol. 311:463–482.

Macpherson J, Wiesendanger M, Marangoz C, Miles TS. 1982. Corticospinal neurones of the supplementary motor area of monkeys. A single unit study. Exp Brain Res. 48:81–88.

Macpherson JM, Marangoz C, Miles TS, Wiesendanger M. 1982. Microstimulation of the supplementary motor area (SMA) in the awake monkey. Exp Brain Res. 45:410–416.

Maier MA, Armand J, Kirkwood PA, Yang HW, Davis JN, Lemon RN. 2002. Differences in the corticospinal projection from primary motor cortex and supplementary motor area to macaque upper limb motoneurons: an anatomical and electrophysiological study. Cereb Cortex. 12:281–296.

Matelli M, Luppino G, Rizzolatti G. 1991. Architecture of superior and mesial area 6 and the adjacent cingulate cortex in the macaque monkey. J Comp Neurol. 311:445–462.

McKiernan BJ, Marcario JK, Karrer JH, Cheney PD. 1998. Corticomotoneuronal postspike effects in shoulder, elbow, wrist, digit, and intrinsic hand muscles during a reach and prehension task. J Neurophysiol. 80:1961–1980.

Mitz AR, Wise SP. 1987. The somatotopic organization of the supplementary motor area: intracortical microstimulation mapping. J Neurosci. 7:1010–1021.

Mushiake H, Inase M, Tanji J. 1991. Neuronal activity in the primate premotor, supplementary, and precentral motor cortex during visually guided and internally determined sequential movements. J Neurophysiol. 66:705–718.

Park MC, Belhaj-Saif A, Cheney PD. 2000. Chronic recording of EMG activity from large numbers of forelimb muscles in awake macaque monkeys. J Neurosci Methods. 96:153–160.

Park MC, Belhaj-Saif A, Cheney PD. 2004. Properties of primary motor cortex output to forelimb muscles in rhesus macaques. J Neurophysiol. 92:2968–2984.

Park MC, Belhaj-Saif A, Gordon M, Cheney PD. 2001. Consistent features in the forelimb representation of primary motor cortex in rhesus macaques. J Neurosci. 21:2784–2792.

Penfield W, Welch K. 1951. Supplementary motor area of the cerebral cortex. Arch Neurol Psychiatry. 66:289–317.

Porter R, Lemon RN. 1993. Corticospinal function and voluntary movement. Oxford: Clarendon Press.

Ranck JB, Jr. 1975. Which elements are excited in electrical stimulation of mammalian central nervous system: a review. Brain Res. 98:417–440.

Rattay F. 1999. The basic mechanism for the electrical stimulation of the nervous system. Neuroscience. 89:335–346.

Rouiller EM, Moret V, Tanne J, Boussaoud D. 1996. Evidence for direct connections between the hand region of the supplementary motor area and cervical motoneurons in the macaque monkey. Eur J Neurosci. 8:1055–1059.

Russo GS, Backus DA, Ye S, Crutcher MD. 2002. Neural activity in monkey dorsal and ventral cingulate motor areas: comparison with the supplementary motor area. J Neurophysiol. 88:2612–2629.

Sakai H, Woody CD. 1988. Relationships between axonal diameter, soma size, and axonal conduction velocity of HRP-filled, pyramidal tract cells of awake cats. Brain Res. 460:1–7.
Shima K, Tanji J. 1998. Both supplementary and presupplementary motor areas are crucial for the temporal organization of multiple movements. J Neurophysiol. 80:3247–3260.
Stoney SD, Jr., Thompson WD, Asanuma H. 1968. Excitation of pyramidal tract cells by intracortical microstimulation: effective extent of stimulating current. J Neurophysiol. 31:659–669.
Takada M, Tokuno H, Hamada I, Inase M, Ito Y, Imanishi M, Hasegawa N, Akazawa T, Hatanaka N, Nambu A. 2001. Organization of inputs from cingulate motor areas to basal ganglia in macaque monkey. Eur J Neurosci. 14:1633–1650.
Tanji J, Shima K. 1994. Role for supplementary motor area cells in planning several movements ahead. Nature. 371:413–416.
Tehovnik EJ. 1996. Electrical stimulation of neural tissue to evoke behavioral responses. J Neurosci Methods. 65:1–17.
Tehovnik EJ, Tolias AS, Sultan F, Slocum WM, Logothetis NK. 2006. Direct and indirect activation of cortical neurons by electrical microstimulation. J Neurophysiol. 96:512–521.
Tokuno H, Nambu A. 2000. Organization of nonprimary motor cortical inputs on pyramidal and nonpyramidal tract neurons of primary motor cortex: an electrophysiological study in the macaque monkey. Cereb Cortex. 10:58–68.
Tokuno H, Tanji J. 1993. Input organization of distal and proximal forelimb areas in the monkey primary motor cortex: a retrograde double labeling study. J Comp Neurol. 333:199–209.
Woolsey CN, Settlage PH, Meyer DR, Sencer W, Hamuy TP, Travis AM. 1952. Patterns of localization in precentral and "supplementary" motor area and their relation to the concept of a premotor area. Assoc Res Nerv Ment Dis. 30:238–264.